DENSE DEFORMATION FIELD ESTIMATION FOR ATLAS REGISTRATION USING THE ACTIVE CONTOUR FRAMEWORK

Valérie Duay, Meritxell Bach Cuadra, Xavier Bresson and Jean-Philippe Thiran

Signal Processing Institute (ITS)
Ecole Polytechnique Fédérale de Lausanne (EPFL)
CH-1015 Lausanne, Switzerland
Email: {valerie.duay, meritxell.bach, xavier.bresson, jp.thiran}@epfl.ch
http://lts5www.epfl.ch/

ABSTRACT

In this paper, we propose a new paradigm to carry out the registration task with a dense deformation field derived from the optical flow model and the active contour method. The proposed framework merges different tasks such as segmentation, regularization, incorporation of prior knowledge and registration into a single framework. The active contour model is at the core of our framework even if it is used in a different way than the standard approaches. Indeed, active contours are a well-known technique for image segmentation. This technique consists in finding the curve which minimizes an energy functional designed to be minimal when the curve has reached the object contours. That way, we get accurate and smooth segmentation results. So far, the active contour model has been used to segment objects lying in images from boundary-based, region-based or shape-based information. Our registration technique will profit of all these families of active contours to determine a dense deformation field defined on the whole image. A well-suited application of our model is the atlas registration in medical imaging which consists in automatically delineating anatomical structures. We present results on 2D synthetic images to show the performances of our non rigid deformation field based on a natural registration term. We also present registration results on real 3D medical data with a large space occupying tumor substantially deforming surrounding structures, which constitutes a high challenging problem.

1. INTRODUCTION

Atlas-based segmentation of medical images has become a standard paradigm for exploiting prior anatomical knowledge in image segmentation (see [1] and [2] for reviews). In the majority of approaches proposed so far to register an atlas to a patient image, the objective of the transformation is to optimize some global intensity-based correspondence measure like gray-level differences or mutual information. The main limitation of these methods is that they often lead to a compromise between the accuracy of the resulting segmentation and the smoothness of its contours. When at some places contours are not accurate enough, a widely used solution is to allow globally or locally more elasticity to the deformation in order to obtain more local deformation (see for instance [3], [4], [5]) with the risk of increasing the irregularity of the deformation field and thus of the contours. Moreover, this does not assure that the sought level of precision will be obtained. To cope with this problem, more local constraints have to be included in the atlas registration process. These constraints should permit the registration on relevant structures, to impose the smoothness of the contours and to introduce more prior knowledge such as the intensity distribution or the admissible shapes of the objects selected to drive the registration. Among the different techniques proposed so far in image analysis, the active contour framework seems to be particularly well appropriated to define and implement such constraints even if it was initially designed for image segmentation.

Hence, we propose in this paper a formulation adapting the active contours segmentation framework to atlas registration. This formalism is derived from the combination of the general level set-based segmentation with the optical flow model. This is not the first attempt of using level set functions in non rigid registration. For example, Paragios et al. proposes in [6] to use the level set function representation in the registration of 2D geometric shapes. To this end, they determine global transformations and a local deformation field in a narrow band around the shape to be registerd. We consider in this paper a different approach, borrowed from atlas-based segmentation in medical imaging ([1], [2]), because a dense deformation field will be determined on the whole image to register the two images. Hence, the registration objective is to get a point to point correspondence between both images and not between shape contours like in [6]. In [7], Leow et al. also proposes to use level set methods to register sulcal curves on cortical surface 2D maps. In their work, they need to use two level set functions to represent the curves of interest. Their evolution equation is thus very specific to curve registration and was only tested on 2D images. In [8], Vemuri et al. propose a registration algorithm based on the level sets of the given images. The registration model presented in this paper borrows the idea of level sets registration of Vemuri at al. but the fundamental and essential difference lies on the registered images. Indeed, the authors of [8] apply the level sets registration on the gray-level intensities of the images to be registered whereas we apply the level sets registration on the level set functions of Osher and Sethian [10] in order to use the numerous segmentation models developed in the level set framework. The paper is organized as follow. Firstly, the general evolution equation for level sets-based registration based on the optical flow model is presented. Then we present a natural speed term directly derived

This work is supported by the Swiss National Science Foundation under grant nbr 205320-101621, the Center for Biomedical Imaging (CIBM) of the Geneva - Lausanne Universities and the EPFL, and the foundations Leenaards and Louis-Jeantet. All this registration process has been implemented in the ITK environment (www.itk.org).

from this new framework. Results will show that this simple speed term is able to model a large range of deformations in medical imaging. In a preliminary work [11] we have already introduced this term to model one type of deformation. We show in this paper that it was actually a particular solution of the general formulation of level set-based registration presented here.

2. METHOD

2.1 Active contour in the level set framework

In the active contour framework, two types of methods have been defined depending of the considered curve parametrization.

The first type called snake methods [9] proposes to parameterize the contours by a linear combination of basis functions (e. g. splines, wavelets, ...) as follows:

$$C(x) = \sum_{i=o}^{k} p_i b_i(x), \tag{1}$$

where $C(x)$ is the parameterized curve at image point x, p_i are the control points, b_i the basis functions and k the number of basis function. The evolution of snake contours is given by the displacement vectors of its control points, namely:

$$\frac{\partial C(x)}{\partial t} = \beta \overrightarrow{N}, \tag{2}$$

where β is the velocity of the flow (or speed term) and $\vec{N}$ is the unit normal to the curve C.

The second type called level set methods [10] proposes to parameterize the contours with a signed distance map (level set function) as:

$$\varphi(x) = \begin{cases} 0 & \text{x} \in C \\ -d(x) & \text{x} \in \Omega_{int} \\ +d(x) & \text{x} \in [\Omega - \Omega_{int}], \end{cases} \tag{3}$$

where $\varphi(x)$ is the level set function at image point x, d is the distance to the closest contour, Ω_{int} is the image area inside the contour and $[\Omega - \Omega_{int}]$ is the image area outside the contour.

The level set function can be seen as the map of the arrived times of an evolutive curve C(t):

$$\varphi(C(t),t) = 0. \tag{4}$$

By deriving (4) with the chain rule and by combining the result with (2), we obtain the active contour evolution equation corresponding to the level set representation:

$$\underbrace{\frac{\delta\varphi}{\delta C}}_{\nabla\varphi}\underbrace{\frac{\partial C}{\partial t}}_{\beta\overrightarrow{N}} + \frac{\partial\varphi}{\partial t} = 0 \Rightarrow \frac{\partial\varphi}{\partial t} = \beta\|\nabla\varphi\|. \tag{5}$$

Note that the unit normal vector $\vec{N}$ is here defined for each isophote, i.e. curve with the same intensity:

$$\overrightarrow{N} = -\frac{\nabla\varphi}{\|\nabla\varphi\|}. \tag{6}$$

The main advantage of the level set representation compared to the snake one is its non parametric nature.

Due to its implicit representation and global contour description, we consider that the level set function representation is a good support to estimate a deformation field defined on the whole image domain.

2.2 Deformation field derived from the optical flow and the level set approach

The dense deformation field we need in registration is extracted by tracking the level set function motion. For that, we use the optical flow method. We choose this voxel-based technique, well-known in image analysis, because it suits well the non parametric nature of the level set representation (for a detailed survey of optical flow methods, see Barron et al. [12]).

The optical flow method is based on the assumption that the brightness of the moving image, here the level set function $\varphi(x,t)$, stays constant for little displacements and a short period of time:

$$\varphi(x,t) = \varphi(x+\vec{u},t+dt) \Rightarrow \frac{d\varphi(x,t)}{dt} = 0 \tag{7}$$

where $\vec{u}$ is the deformation vector field.

The optical flow constraint (7) can thus be rewritten as:

$$\bigtriangledown\varphi(x,t)\frac{\partial\vec{u}}{\partial t} + \frac{\partial\varphi(x,t)}{\partial t} = 0. \tag{8}$$

From (8) we get the evolution equation of the vector flow:

$$\frac{\partial\vec{u}}{\partial t} = -\frac{\varphi_t}{\|\bigtriangledown\varphi(x,t)\|}\frac{\bigtriangledown\varphi(x,t)}{\|\bigtriangledown\varphi(x,t)\|}, \tag{9}$$

where φ_t represents the variation of the level set function according to the desired application such as segmentation, registration, regularization, ...

2.3 General formulation of level set-based registration

The vector flow equation (9) obtained by applying the optical flow assumption on level set functions and the general formulation of the level set-based framework (5) are as follows:

$$\begin{cases} \frac{\partial\vec{u}}{\partial t} = -\frac{\varphi_t}{\|\bigtriangledown\varphi(x,t)\|}\frac{\bigtriangledown\varphi(x,t)}{\|\bigtriangledown\varphi(x,t)\|} & \text{(a)} \\ \varphi_t = \beta\|\nabla\varphi(x,t)\| & \text{(b).} \end{cases} \tag{10}$$

By combining these two equations (replace φ_t of (10(a)) by (10(b))), we obtain the following formulation generalizing the active contours framework to image registration:

$$\frac{\partial\vec{u}}{\partial t} = -\beta\frac{\bigtriangledown\varphi(x,t)}{\|\bigtriangledown\varphi(x,t)\|}. \tag{11}$$

In this new framework, the deformation field is the important variable and not anymore the contour as in the standard active contour framework. However, our registration model keeps the same advantages of level set-based segmentation in term of accuracy, prior knowledge and regularization constraints for the same computation cost. In fact, all the evolution terms designed for the segmentation can be reused for image registration. The new level set-based registration framework involves now to develop new terms based on two images, the moving and the fixed images. The next section presents an evolution term specially designed for this purpose.

2.4 A natural registration term

The active contour evolution stops when it reaches the desired object contours, i.e. $\varphi(x,t) = \varphi_T(x)$, where $\varphi(x,t)$ is the active contour and $\varphi_T(x)$ is the target contours. Thus, a natural speed term would be $\varphi_T(x) - \varphi(x,t)$. Hence, the equation (11) becomes:

$$\frac{\partial \vec{u}}{\partial t} = -(\varphi_T(x) - \varphi(x,t)) \frac{\bigtriangledown \varphi(x,t)}{\| \bigtriangledown \varphi(x,t) \|} \tag{12}$$

with $\varphi(x,0) = \varphi_S(x)$, where $\varphi_S(x)$ is the source contours.

Besides, the current level set function $\varphi(x,t)$ is related to the original level set function $\varphi_S(x)$ by the extracted deformation field $\vec{u}$ in the following way:

$$\varphi(x,t) = \varphi_S(x - \vec{u}). \tag{13}$$

Note that the level set function carried over by the current deformation field, the property of signed distance function will be violated as soon as the registration starts and thus causes numerical inaccuracy. In order to avoid this, the level set function $\varphi(x,t)$ has to be re-initialized at each iteration. The total deformation field at each iteration is discretized as follows:

$$\vec{u}(t+1) = \vec{u}(t) + \frac{\partial \vec{u}(t)}{\partial t}. \tag{14}$$

where $\vec{u}(t)$ is the deformation field at time t.

Fig. 1 shows an illustration example. Fig. 1(a) and 1(b) respectively show a binary source and target images representing a sad and a happy face. The objective is to register the sad face to the happy face. 1(c) and 1(d) are the level set functions corresponding to these images. Fig. 1(f) shows the direction of the vector flow estimated by the normalized gradient of $\varphi(x,t)$. Fig. 1(e) shows the magnitude of the displacement estimated by the difference between the two signed distance map $\varphi_T(x)$ and $\varphi(x,t)$. The white areas correspond to extension motions, black areas to contraction motions and gray uniform areas to areas without motion. The extracted deformation field is globally quite smooth (see Fig. 1(g)). This is due to the fact that the displacement generated by the contours is perpendicular to the contour following the direction of the gradient (see Fig. 1(f)). Therefore, discontinuities appear on the skeleton of the image where two fronts reach themselves. Inspired by the optical flow regularization, a Gaussian filtering is applied on the deformation field at the end of each iteration. This permits to remove discontinuities while propagating the correction to the whole image (see Fig. 1(h)). The Gaussian filtering necessitates to set a parameter σ. This parameter permits to limit the maximal elasticity of the deformation.

Therefore, the equation 14 becomes:

$$\vec{u}(t+1) = (\vec{u}(t) + \frac{\partial \vec{u}(t)}{\partial t}) \circ G(\sigma). \tag{15}$$

We would like to make clear here that future work include to replace this gaussian filtering-based regularization by adding a mean curvature regularization term in the evolution equation.

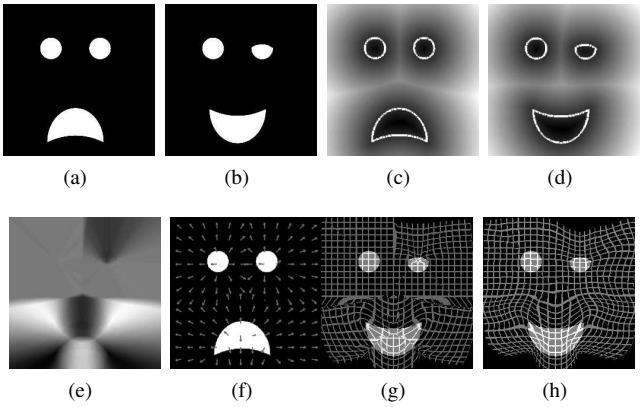

Figure 1: Deformation field extraction process on 2D synthetic data: (a) and (b) are the source and target binary images, (c) and (d) are their corresponding level set functions, (e) is the difference between the target level set function and the moving level set function (magnitude of the displacement), (f) is the normalized gradient computed on the moving level set function (direction of the displacement), (g) is the grid deformation without gaussian regularization, and (h) the grid deformation with a gaussian regularization.

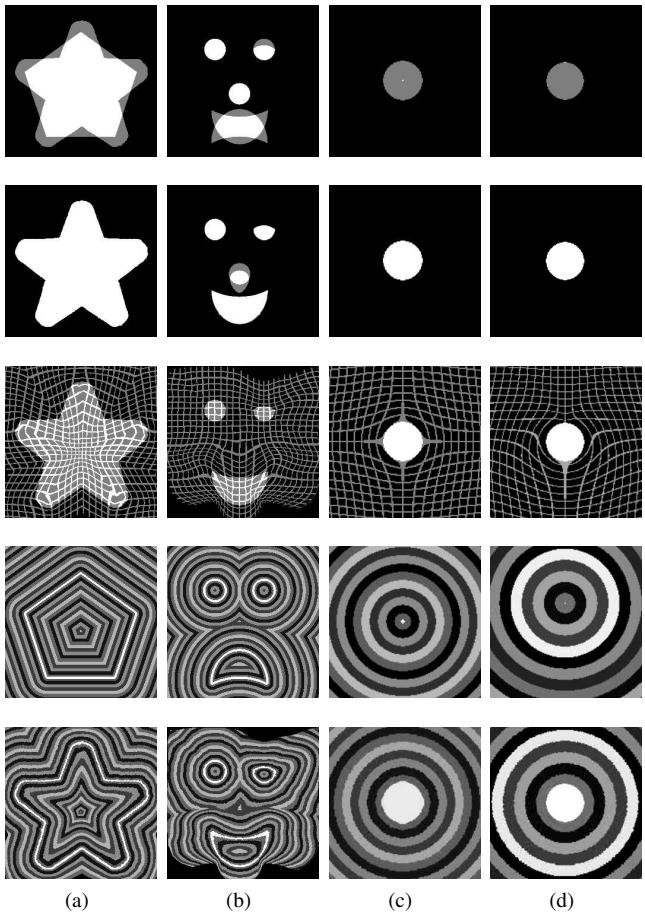

Figure 2: Deformation field extracted from different type of objects. Row (1): Initial difference. Row (2): Final difference. Row (3): Deformed regular grid. Row (4): Test image. Row (5): Deformed test image.

3. RESULTS

3.1 Synthetic images

Our natural registration term is first evaluated to recover non rigid deformations between 2D synthetic binary images.

Each column of Fig. 2 presents the results obtained on mono-

component objects, multi-components objects and on the deformation of a point to a disc. This last experiment represents a new contribution. So far, one level set function was always used to represent closed contours and not points. Here the point is in fact represented by a normal distance map (not signed). At each column, row 1 shows initial differences between the source and the target images (common sections are shown in white, regions that do not correspond are shown in gray). Row 2 shows these differences after having deformed the source image with the extracted non rigid transformation. Row 3 shows the transformation applied to a regular grid. Row 4 shows the modulo distance map of the source image (object contours are enhanced in white). Row 5 shows the test image of row 4 deformed with the computed transformation. The few gray regions of row 2 shows the accuracy of contour matching on 2D images. For the second case concerning face expressions, we note a difference on the nose. This registration was only based on the features defined by the eyes and the mouth. Thus, the nose of the source image has just followed the computed transformation. The deformed grid and the test image of rows 3 and 5 help in visualizing the regularity of the computed transformations. For the point matching experiment, the grid well show the differences in the deformation when the point is placed in the center of the disc or on a extremity. In the first case, the deformation induced is radial with the same intensity in all direction. For the second case, the deformation is also radial but strongest at the opposite extremity of the disc and fades more we move away from this position. These synthetic examples can be related to particular applications in medical image registration. The first one corresponds to the registration of closed structures, the face matching experiment illustrates the estimation of non visible objects position from the local registration of visible objects and the point matching could model a tumor growth in an atlas. The next section presents preliminary results on real data for these three applications.

3.2 Real data

The real application concerns the registration of an atlas on a brain presenting a large-space occupying tumor. Such registration is challenging because: (1) the lesion does not exist in the atlas, (2) large deformations have to be recovered. However we decide to use this case for our prelimary results on real data because we can model two types of deformations: surface matching and tumor growth by matching a point (seed) to a volume (segmented tumor). First, the atlas was registered to the volume of interest with a twelve degrees of freedom transformation using a mutual-information based technique (implemented with the ITK registration toolbox) in order to compensate the global differences of position. The patient image used in this study has been retrieved from the Surgical Planning Laboratory (SPL) of the Harvard Medical School & NSG Brain Tumor Database [14]. The digital atlas also comes from the SPL [13].

The features used for the registration can be classified in two categories: 1. Features to limit the propagation of the deformation: head and brain contours. 2. Features to catch the most of the deformation due to the pathology: lateral ventricles and tumor. Two different segmentation techniques are used to segment these features: level set methods for contrasted structures (head and ventricles) and mathematical morphology to extract the brain. The level set-based registration is then performed on the binary images generated by these segmentations.

With this technique, to obtain a correct radial tumor growth, the seed has to be the only object placed inside the tumor area of the patient. As the lateral ventricles overlap this area, they are registered in a second step. So, we have to perform a hierarchical registration process with two layers (first layer: head, brain and tumor, second layer: lateral ventricles) following the approach proposed by Houhou et al. [15].

Fig. 3 shows the difference of position between the source and target binary images used during the registration process for the sagittal view (raw 1) and the axial view (raw 2). Columns 1 and 2 show respectively the initial and final position. We note some gray part in the final difference. These misregistrations are due to the fact that we use a voxel-wise distance maps algorithm to compute the 3D level set functions. More accuracy could be get with sub-voxel distance maps. Another reason comes from the use of a Gaussian filter for the regularization. At each filtering we lost accuracy to get a smoother deformation field. We are currently improving this by using the mean curvature-based regularization term coming from the active contours framework.

The objective of atlas registration is to automatically segment the patient image. The raw 3 of Fig. 3 shows how two other structures of the atlas, the cerebellum and the caudate nucleus (white contours), follow the deformation interpolated from the features registration (gray contours). The column (a) shows the atlas contours superposed to the patient image. The column (b) shows these contours deformed by the computed transformation.

Fig. 4 shows the effect of the tumor growth on the surrounding structures of the atlas. Panel (a) shows the atlas. Panel (b) shows the atlas just after the tumor growing (after the registration of layer 1). Panel (c) shows the patient image. Contours of the tumor and lateral ventricles have been drawn on the patient image and copy on the other panels to show how the structures follow the deformation generated by the tumor growing. We note that the deformation generated by the tumor growth already gives to the lateral ventricles and the corpus callosum a shape similar to the patient's structures.

With this experiment, we wanted to show the effect of the natural registration term only. The limitations of this term are that it necessitates the segmentation of the patient image. Thus we propose to use it when the targeting structures are easy to segment (for example bones in CT images) or to add constrain on manually segmented objects. The results of this term strongly depends of the quality of segmentation of the patient. So this distance-based term should be used with other evolution terms like boundary or region based. Thus eventual segmentation errors could be compensate. Concerning the tumor growth, the generated deformation is related to the position of the seed. Thus, the seed was placed in the atlas following the knowledge of an expert about the real origin of the tumor.

4. CONCLUSION

In this paper, we present a general formulation adapting the active contour framework to atlas registration. It permits to

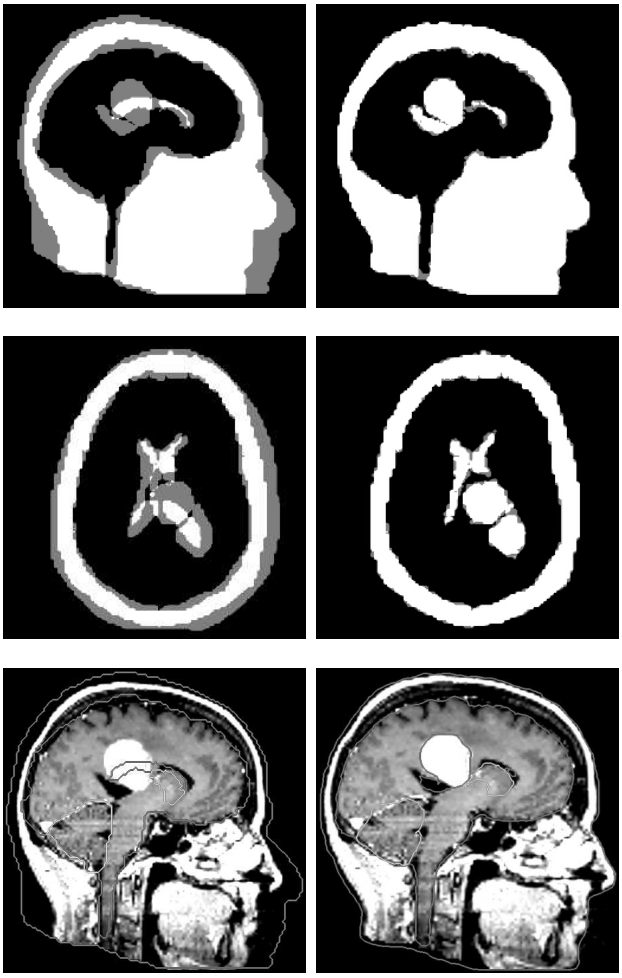

(a) (b)

Figure 3: Geometrical feature-based atlas registration. Row 1: Axial view. Row 2: Sagittal view. Column (a): Initial differences. Column (b): Final differences. Row 3: Atlas based segmentation of a brain image with large tumor. Column (a): Initial atlas contours on patient image. Column (b): Deformed atlas contours.

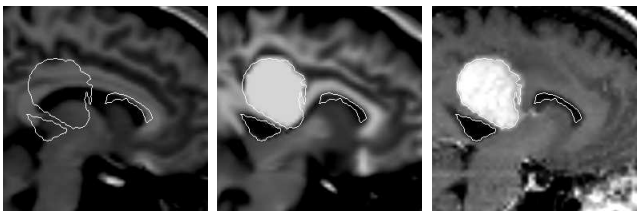

(a) (b) (c)

Figure 4: Tumor growing. (a) Atlas. (b) Atlas deformed. (c) Patient image.

perform a segmentation and registration task in one step, that suit particularly well the atlas registration methods. This new framework implies developing evolution term based on the source and target images. One term based on distance map for geometrical features matching was shown here. We show that it can model different types of deformations present in medical images. Future work include showing the effect of the classical evolution terms designed for active contour segmentation in the registration (curvature-based, boundary-based and region-based). Concerning the atlas registration on brain with large tumor, the future results obtained with our level set-based registration will be compared with the model of tumor growth previously proposed by our lab [16].

REFERENCES

[1] C.R.J. Maurer et al., "A review of medical image registration," *Interactive Image-Guided Neurosurgery*, R. Maciunas, Editor. , American Association of Neurological Surgeons: Park Ridge, IL, pp. 17–44, 1993.

[2] J.B. Maintz et al., "A survey of medical image registration," *Medical Image Analysis*, 2(1), pp. 1–36, March 1998.

[3] J.P. Thirion, "Image matching as a diffusion process: an analogy with Maxwell's demons," *IEEE Transaction on Medical Image Analysis*, 2 (3), pp. 243–260, 1998.

[4] G. K. Rohde et al., "The Adaptive Bases Algorithm for Intensity-Based Nonrigid Image Registration," *IEEE Transactions on Medical Imaging,*, 22(11), pp. 1470–1479, November 2003.

[5] V. Duay et al., "Non-Rigid Registration AlgorithmWith Spatially Varying Stiffness Properties," in *Proc. ISBI04*, Arlington, VA, USA, pp. 408–411, April 2004.

[6] N. Paragios et al., "Non-rigid registration using distance functions," *Computer Vision and Image Understanding*, 89, pp. 142-165, 2003.

[7] A. Leow et al., "Brain Warping with Implicit Representations," in *Proc. ISBI 2004*, Arlington, VA, USA, pp. 603–606, April 2004.

[8] B. C. Vemuri et al., "Image registration via level-set motion : Applications to atlas-based segmentation," *IEEE Transaction on Medical Image Analysis*, 7(1), pp. 1–20, March 2003.

[9] M. Kass et al., "Snakes: active contour models," in *First international conference on computer vision*, pp. 259–268, 1987.

[10] S. Osher and J. A. Sethian, "Fronts propagating with curvature-dependent speed - algorithms based on hamilton-jacobi formulations," *Journal of Computational Physics*, 79(1), pp. 12–49, 1988.

[11] V. Duay et al., "Atlas-Based Segmentation of Medical Images Locally Constrained by Level Sets," in *ICIP05*, Genova, Italia, 2005.

[12] J. L. Barron et al., "Performance of optical flow techniques," *Intl. J. Comput. Vision*, 1(12) pp. 43–77, 1994.

[13] R. Kikinis et al., "A digital brain atlas for surgical planning, model driven segmentation and teaching," *IEEE Trans. on Visual. and Comput*, Graph. 2, 1996.

[14] M. R. Kaus et al., "Segmentation of Meningiomas and Low Grade Gliomas in MRI," *MICCAI99*, pp. 1–10, 1999.

[15] N. Houhou et al., "Medical Images Registration with a Hierarchical Atlas," in *EUSIPCO'05*, 2005.

[16] M. Bach Cuadra et al., "Atlas-based Segmentation of Pathological MR Brain Using a Model of Lesion Growth," *IEEE Transactions on Medical Imaging*, 23 (10), pp. 1301–1314, October 2004.